Climate Dynamics (1997) 13:1–9

Climate Dynamics

The climate of Europe 6000 years ago

R. Cheddadi[1,2], G. Yu[3], J. Guiot[2], S. P. Harrison[3], I. Colin Prentice[4]

[1] European Pollen Database, Centre Universitaire d'Arles, F-13200 Arles, France
[2] Laboratoire de Botanique Historique et Palynologie, CNRS UA 1152, Faculté de St-Jérôme, Case 451, F-13397 Marseille cedex 20, France
[3] Dynamic Palaeoclimatology, Lund University, Box 117, S-221 00 Lund, Sweden
[4] Global Systems Group, Department of Ecology, Lund University, Ecology Building, Sölvegatan 37, S-22362 Lund, Sweden

Received: 3 January 1996 / Accepted: 15 July 1996

Abstract. Palaeoclimates across Europe for 6000 y BP were estimated from pollen data using the modern pollen analogue technique constrained with lake-level data. The constraint consists of restricting the set of modern pollen samples considered as analogues of the fossil samples to those locations where the implied change in annual precipitation minus evapotranspiration ($P-E$) is consistent with the regional change in moisture balance as indicated by lakes. An artificial neural network was used for the spatial interpolation of lake-level changes to the pollen sites, and for mapping palaeoclimate anomalies. The climate variables reconstructed were mean temperature of the coldest month (T_c), growing degree days above 5 °C (GDD), moisture availability expressed as the ratio of actual to equilibrium evapotranspiration (α), and $P-E$. The constraint improved the spatial coherency of the reconstructed palaeoclimate anomalies, especially for $P-E$. The reconstructions indicate clear spatial and seasonal patterns of Holocene climate change, which can provide a quantitative benchmark for the evaluation of palaeoclimate model simulations. Winter temperatures (T_c) were 1–3 K greater than present in the far N and NE of Europe, but 2–4 K less than present in the Mediterranean region. Summer warmth (GDD) was greater than present in NW Europe (by 400–800 K day at the highest elevations) and in the Alps, but >400 K day less than present at lower elevations in S Europe. $P-E$ was 50–250 mm less than present in NW Europe and the Alps, but α was 10–15% greater than present in S Europe and $P-E$ was 50–200 mm greater than present in S and E Europe.

Introduction

Palaeoclimatic proxy data offer the possibility of evaluating the performance of climate models under changed boundary conditions. This insight has spurred attempts to synthesize available proxy data for key times for which climate model experiments have been performed, and to develop reliable tools to translate proxy data into quantitative estimates of climate variables that can be compared with model predictions. Particular interest has focused on the interval around 6000 y BP (^{14}C time scale) (e.g. COHMAP Members 1988; Wright et al. 1993). The millenium around 6000 y BP was approximately the time of maximum summer warmth in many Northern Hemisphere mid- to high-latitude regions, and 6000 y BP lies within the interval of greater than present summer rainfall (monsoon expansion) in northern subtropical regions (Kutzbach and Street-Perrott 1985; COHMAP Members 1988). The time of 6000 y BP is a clear choice from a modelling perspective too, because the conditions of the time can be approximated as a pure orbital forcing experiment, in which continental ice sheet distributions and atmospheric CO_2 concentration are held at their modern or pre-industrial states.

In the present study, pollen data are used to estimate palaeoclimate variables. Pollen data inherently reflect those aspects of climate that influence vegetation, and modern pollen assemblages from Europe are more closely related both causally and statistically to "bioclimatic" variables (such as growing degree days, *GDD,* and the ratio of actual and equilibrium evapotranspiration, (α) than to conventional variables such as annual precipitation that influence vegetation only indirectly (Guiot et al. 1993). In humid temperate regions including much of northern and western Europe, α approaches its maximum value and the vegetation is insensitive or only slightly sensitive to further increases in precipitation. Lake levels by contrast respond to the annual water balance (precipitation minus actual evapotranspiration, $P-E$) over the catchment, and remain sensitive to changes in precipitation even in wet climates (Evans and Trevisan 1995; see Appendix). Guiot et al. (1993) showed that application of a constraint based on lake-level changes gave rise to a decrease in variance and an increase in the spatial coher-

Correspondence to: R. Cheddadi, edp@dialup.francenet.fr

ency of Holocene palaeoclimate reconstructions based on pollen data.

Using a method similar to that established by Guiot et al. (1993), we now present a palaeoclimatic reconstruction of Europe at 6000 y BP based on a substantially expanded data set of pollen assemblages and lake level records. The area considered ranges from 10 °W to 60 °E and 35 °N to 75 °N, encompassing Western and Central Europe, the northern part of the Mediterranean Basin and the western part of the former Soviet Union. The results are intended to represent a state-of-the-art reconstruction based on most of the currently available data, and to be used as a target data set with which model predictions can be compared; for example within the framework of the Paleoclimate Modelling Intercomparison Project (PMIP), for which 6000 y BP is an important focus.

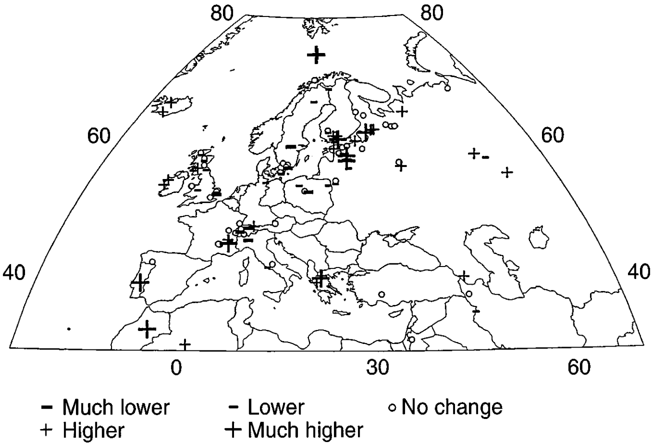

Fig. 1. Lake status anomalies, 6000 y BP minus present

Data

Lake level data

The lake databases covering this area are the European Lake Status Data Base (ELSDB.1: Yu and Harrison 1995a), the Former Soviet Union and Mongolia Lake Status Data Base (FSUDB.1: Tarasov et al. 1994) and the Oxford Lake-level Data Base (OLLDB: Street-Perrott et al. 1989). The documentation for each database includes detailed analysis of the various proxy records used to make the reconstructions and explanations of the logic used to generate the codes entered in the database. Basins with records that show signs of having been influenced by neotectonism, changes in the course of a river, changes in the threshold of the lake overflow, or glacier fluctuations are not includes.

Within the European study area, 134 sites in the relevant data bases have records for 6000 y BP. From these we have selected only those sites which are lakes today, thereby excluding 13 sites where the recent part of the record appears to reflect infilling and/or hydroseral development. We have used the dating control and dating method information in the data bases to exclude sites where either: (a) dating control is poor (dating control >4, i.e. sites where there is only a single radiocarbon date, it is more than 1000 y from the 6000 y BP target date, or, in situations of continuous sedimentation with bracketting radiocarbon dates, both radiocarbon dates are further than 4000 y from the target date); or (b) the dating is based entirely on correlation with regional stratigraphic, biostratigraphic or archaeological schemes (dating method control >3). Finally 110 sites were retained. For each site, lake level was expressed as a semi-quantitative anomaly variable (lake status) taking integer values from -2 (much lower than present) to $+2$ (much higher than present) (Fig. 1). Low lake levels occur in the region around the Baltic and North Sea, in the Alps and in the Middle East, while high lake levels occur along the northern and western seaboards, in Northern Europe east of the Baltic, and in the mountains of Southern Europe.

Modern pollen data

The modern pollen data consist of 1331 pollen assemblages from surface deposits from Europe, N Asia and N Africa between 10°W and 100°E, and 30°N and 80°N, i.e. the surface pollen spectra used in Guiot (1990) with supplementary data from Huntley and Birks (1983) and Peterson (1983), plus 148 pollen assemblages from tundra and cool steppe vegetation in North America (P. J. Bartlein, personal communication 1995). The inclusion of data from a wider area than is considered for 6000 y BP is important in order to increase the possibilities of finding appropriate analogues for past climates. Pollen percentages were calculated relative to the sum of 44 pollen types [*Abies, Acer, Alnus, Betula, Buxus, Carpinus, Castanea, Cedrus, Corylus, Ephedra, Fagus, Frangula, Fraxinus excelsior, F. ornus, Hippophae, Ilex, Hedera, Juglans, Juniperus, Larix, Lonicera, Olea, Ostrya, Phillyrea, Picea, Pinus* (Diploxylon), *Pinus* (Haploxylon), *Pistacia, Platanus, Populus, Quercus* (deciduous), *Quercus* (evergreen), *Rhus, Salix, Taxus, Tilia, Ulmus, Viscum, Vitis, Artemisia,* Chenopodiaceae, Cyperaceae, Ericaceae, Poaceae].

6000 y BP pollen data

The 6000 y BP pollen data consist of the 310 pollen spectra of Huntley and Birks (1983) used in Guiot et al. (1993), and an additional 93 from the European Pollen Database (EPD) (Fig. 2). Among these sites, the 6000 y BP time marker was assigned based on interpolating between ^{14}C dates or by biostratigraphic correlation with nearby ^{14}C-dated sites. The EPD sites fill important gaps especially in the Mediterranean basin, which was poorly represented in the Huntley and Birks (1983) compilation. Pollen percentages were cal-

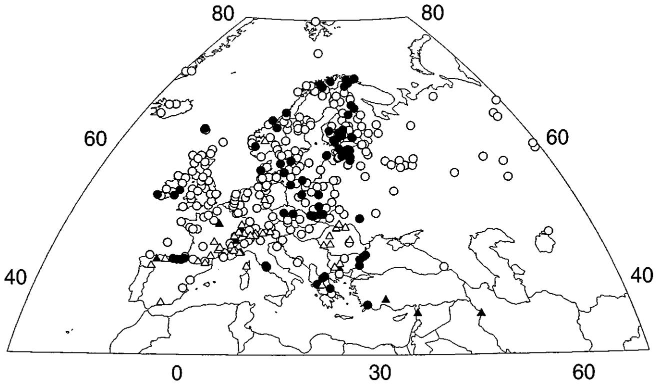

Fig. 2. Pollen sites at 6000 y BP. *Open symbols* represent sites from Huntley and Birks (1983), *closed symbols* sites from the European Pollen Database. Sites at over 1000 m elevation are indicated with *triangles,* other sites with *circles*

culated relative to the same 44 pollen types as were used for the modern data.

Modern climate data

The following modern climate variables were estimated for each modern and 6000 y BP pollen site: mean temperature of the coldest month (T_c), growing-degree days above 5 °C (GDD), the ratio of annual actual to annual equilibrium evapotranspiration (α), and total annual precipitation minus actual evapotranspiration (P–E). These variables were selected in preference to a standard set of variables, such as mean July and January temperature and precipitation, because of their more direct relationships to the factors governing vegetation composition or lake levels. Their values were calculated by B. Huntley (personal communication 1993) from the latitude, longitude and elevation of each site. This calculation involved a two-step procedure, first using the climate data set and interpolation procedure of Leemans and Cramer (1991) in order to obtain long-term monthly means of temperature, precipitation and fractional sunshine hours, then applying algorithms from the BIOME model of Prentice et al. (1992a) to compute GDD and actual to equilibrium evapotranspiration. All of the bioclimatic variables were calculated from monthly means and then interpolated between the mid-months to yield quasi-daily values, as in Prentice et al. (1992a). Soil water capacity was specified from gridded soil texture class data as in Prentice et al. (1992a).

Methods

The analogue technique

The techniques now in use to translate quantitative terrestrial proxy data (such as pollen and beetle assemblages) into quantitative palaeoclimatic estimates are all variants of the modern analogue approach. The degree of analogy between modern and 6000 y BP pollen assemblages was measured with chord distance (Overpeck et al. 1985; Guiot 1990; Prentice et al. 1991), i.e. the Euclidean distance between pollen assemblages after square-root transformation of the pollen percentages. For each fossil pollen assemblage, the eight most similar modern assemblages were taken as "best analogues" provided their distance was less than 0.4, a threshold value obtained by Monte Carlo simulation (Guiot 1990).

Table 1. Correlations between modern pollen-inferred and observed values of climate variables at the modern pollen sampling sites

Variable	Correlation (r)
T_c	0.90
GDD	0.83
α	0.86
$P-E$	0.75

The quality of the reconstructions was assessed by using modern pollen assemblages to estimate the climatic variables and comparing the results to the true values for each assemblage (Table 1). All the correlations were acceptable, but P–E had a lower correlation (0.75) than the other variables (>0.80).

Interpolation of lake status anomalies

As the lake sites are generally at different locations from the pollen sites, it was necessary to develop an interpolation method to estimate lake status at the pollen sites. We used an artificial neural network (ANN). An ANN consists of a number of simple interconnected processors called neurodes (Caudill and Butler 1992). A signal coming from input variables passes through these neurodes to reach the output variables. The architecture of the ANN is composed of a set of layers, each layer consisting of a number of neurodes. At each neurode, the incoming signal is transformed by a non-linear function. The interconnections among neurodes are defined by coefficients that are iteratively adjusted until they optimally fit the output variables, through a process called "training" for which various algorithms exist. We used the backpropagation algorithm as in Guiot et al. (1996) with geographic coordinates as the input variables, and the lake status anomaly for 6000 y BP as the output variable. The ANN was developed using the 110 observations. A stable sum of squared errors was reached after 20000 iterations. The correlation between estimated and observed values of the lake status anomaly was then 0.73. Elevation was not taken into account in this interpolation (a) because some pollen sites are at a very high elevation, implying a risk of spurious extrapolation when there is no lake site at an equivalent elevation, and (b) because lakes (especially in mountain regions) commonly reflect catchment water balance at higher elevations.

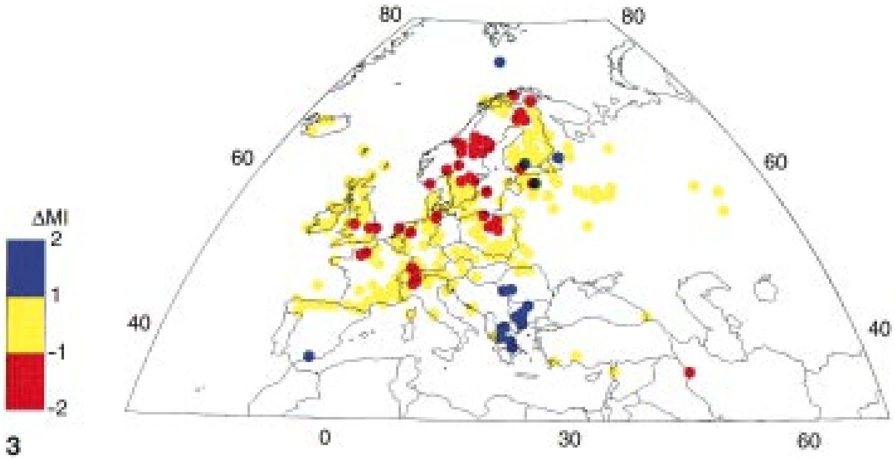

Fig. 3. Lake status anomalies (ΔMI) interpolated to the pollen sites, 6000 y BP minus present

Lake status anomalies were estimated for the 403 sites with 6000 y BP pollen data (Fig. 3). However, 61 pollen sites were found to be more than 5° from a lake site. For these pollen sites it was assumed that the lake status anomaly remains unknown, and no constraint could be applied. The interpolated lake status anomalies are referred to below as ΔMI (change in moisture index), following Guiot et al. (1993).

Rationale and application of the constraint

The method of constraining the analogue reconstruction differs only in a few small ways from that explained in detail by Guiot et al. (1993). The most important change is that the lake status anomalies are now compared with P–E, rather than with precipitation minus potential evaporation ($P-E_p$) as in Guiot et al. (1993). This change was made because lake level changes, especially in humid regions, are expected theoretically to reflect changes in $P-E$ more closely and monotonically than changes in $P-E_p$ (see Appendix). The presence of an outlet in overflowing lakes reduces but does not eliminate the sensitivity of lake level to further increases in $P-E$.

The procedure summarized next was carried out for each of the 403 pollen assemblages from 6000 y BP:
1. Select as analogues all modern pollen assemblages with chord distance <0.4, based on the pollen data alone.
2. Compute $\Delta(P-E)$ for each of these modern assemblages, as the difference between their $P-E$ values and the modern $P-E$ value interpolated to the location of the 6000 y BP pollen site.
3. Reject those modern pollen assemblages with $\Delta(P-E)$ values inconsistent with the lake-derived value of ΔMI, according to the following consistency criteria:

$$-1<\Delta MI<1 \Rightarrow \Delta(P-E)\in[-150, 150 \text{ mm}]$$
$$\Delta MI>1 \Rightarrow \Delta(P-E)>50 \text{ mm}$$
$$\Delta MI<-1 \Rightarrow \Delta(P-E)<-50 \text{ mm}$$

The constrained analogues are those that remain after modern pollen assemblages that do not satisfy these criteria have been rejected.
4. Use the eight best constrained analogues to reconstruct the climatic variables of interest. If there are fewer than eight analogues with chord distance values lower than 0.4, the estimates are based on a reduced number of analogues.

Coherency analysis

It is impossible to check directly with the modern data which method (constrained or unconstrained) is better for each climatic variable, because the constraints are not specified for the present day. Instead we assume that the more reliable method will be the one that yields the more *spatially coherent* palaeoclimate anomaly pattern. We therefore calculated correlations (for each climate variable) between (a) the reconstructed palaeoclimate anomaly values at the 403 sites, and (b) interpolated anomaly values, obtained by averaging the anomaly values for surrounding sites weighted by the inverse of the distances between the sites (Table 2). GDD, T_c and α showed modest increases (<0.1) in coherency due to the constraint. $P-E$ showed a much larger increase (0.25), as might be expected since this variable relates more closely to lake-level changes than to vegetation changes.

Table 2. Spatial coherency (correlation between individual site reconstructions and inverse-distance weighted averages for the surrounding sites) for constrained and unconstrained 6000 y BP climate reconstructions

Variable	Pollen (unconstrained)	Pollen + lakes (constrained)
T_c	0.55	0.60
GDD	0.55	0.60
α	0.60	0.69
$P-E$	0.47	0.72

Table 3. Modern pollen-inferred minus observed values of climate variables for modern pollen sampling sites in different elevation bands

Elevation (m)	T_c (K)	*GDD* (K day)	α (%)	$P-E$ (mm)	Sample size
0–500	−0.1	− 72	+0.2	+ 6	879
500–1000	−0	−206	+1.1	− 4	171
1000–1500	−0	+ 91	−0.6	− 15	136
1500–2000	+0.7	+242	−1.7	− 64	95
2000–2500	+1.3	+449	−6.3	−163	32
>2500	+2.1	+409	+3.6	− 45	18

Removal of elevation bias

Table 3 indicates that there is an elevation-related bias in climate reconstructions from the modern assemblages. This may be partly a statistical artefact (the method is more likely to choose analogue samples that are from climates warmer and drier than those at high elevations simply because such climates are better represented in the data set) and partly due to the problem of upslope pollen transport, which may make pollen assemblages from mountains more reflective of downslope conditions (Huntley 1994). To correct for this bias we recalculated anomalies relative to the reconstructed modern climates, instead of actual modern climates, for all pollen sites above 1000 m.

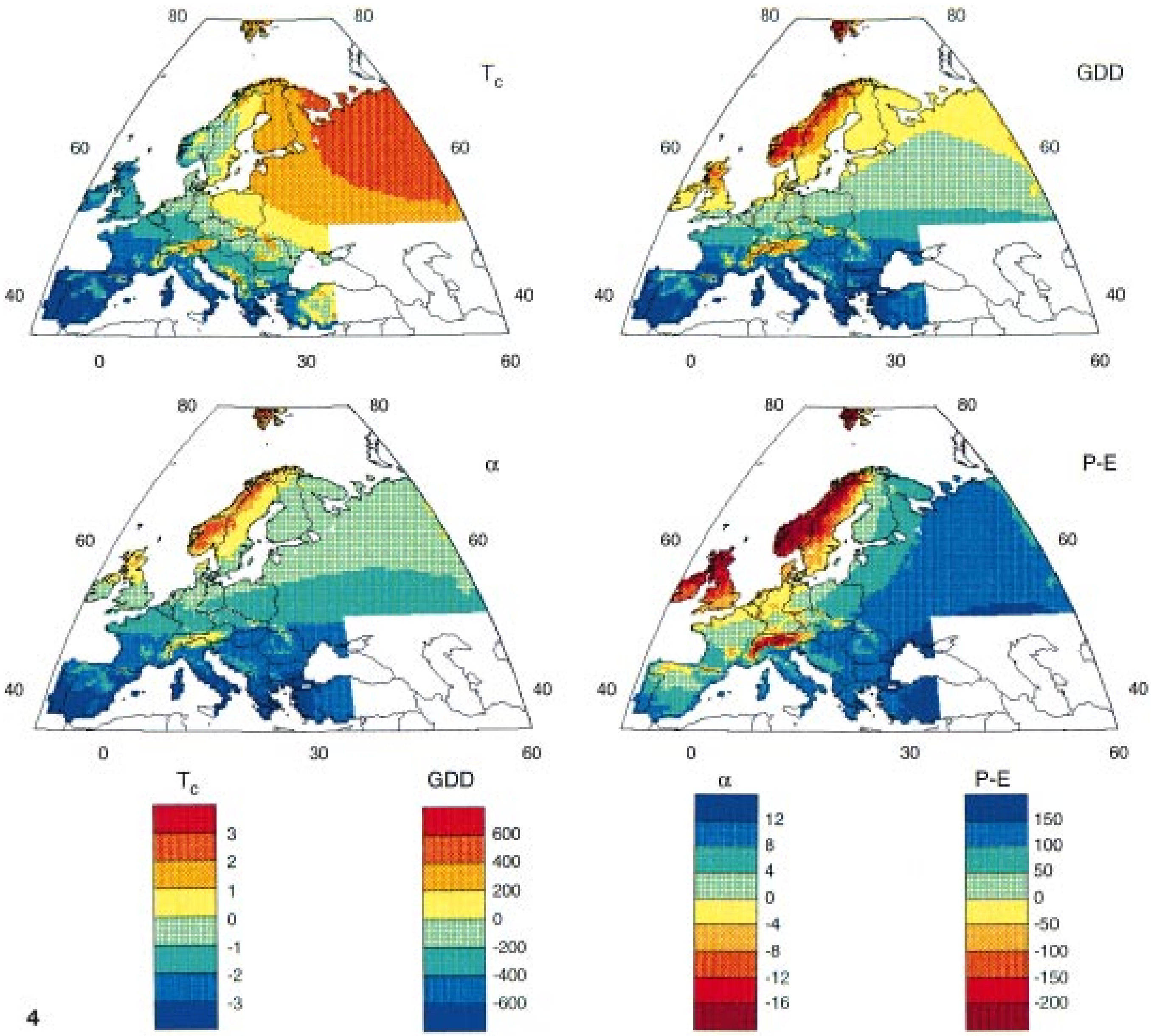

Fig. 4. Constrained-analogue reconstruction of climate anomalies, 6000 y PB minus present. T_c in K, *GDD* in K day, α in % and $P-E$ in mm

Mapping anomaly values and their significance

The anomaly values (relative to actual modern climate for sites below 1000 m, relative to reconstructed modern climate for sites above 1000 m) were interpolated three-dimensionally using the ANN method, with input variables latitude, longitude and elevation (Fig. 4). A non-parametric measure of the significance of each anomaly value was calculated as follows:

$$\Delta^* y(i) = 2\,\Delta y(i) / [y_{\max}(i) - y_{\min}(i)]$$

where $\Delta y(i)$ is the estimated anomaly of climate variable y at site i, and $y_{\max}(i)$ and $y_{\min}(i)$ are the largest and smallest values of climate variable y associated with the set of best constrained analogues for site i. $\Delta^* y(i)$ takes values outside the range $[-2, 2]$ whenever the absolute magnitude of the estimated climate anomaly exceeds the total climatic range of the analogues. This is a conservative criterion for the significance of the anomalies.

Values of $\Delta^* y(i)$ were interpolated to the 0.5° grid using the ANN. Figure 5 shows regions with interpolated values lying outside the range $[-2, 2]$. In Fig. 6, the reconstructed anomalies are shown only for these regions. Figure 6 thus highlights the anomaly values for those regions where a high degree of confidence can be placed in the existence of a *change* in climate between 6000 y BP and present.

Results

Reconstructed winter temperatures (T_c) were up to 3 K greater than present in the far north (northernmost Fennoscandia, Svalbard) and also in northern Russia, implying a reduced west-east gradient across Northern Europe. In contrast, winters were 2–4 K colder than present in the Iberian peninsula, S France and generally around the northern Mediterranean seaboard.

Growing degree days (*GDD*) show a distinctly different pattern, with values greater than present across NW Europe (N Britain and Scandinavia) and in the Alps. The largest positive anomalies (400–800 K day) occur at high elevations in both regions. High *GDD* values in NW Europe, combined with small and non-significant changes in winter temperature, imply that summer temperatures must have been greater than present. High *GDD* values in the far north may also in part reflect longer growing seasons, consistent with the reconstructed relative mildness of the winters. On the other hand, with the exception of the highest mountain regions, *GDD* values in S Europe generally were >400 K day lower than present. Low *GDD* in S Europe may have been due to low summer temperatures and/or shorter thermal growing seasons, consistent with the reconstructed coldness of the winters.

Both precipitation minus evapotranspiration ($P-E$) and the moisture availability index α show a pattern of wetter than present conditions at lower elevations across S and E Europe, constrasting with drier than present conditions in the far north and northwest of Europe and in the Alps. The indication of dry land-surface conditions (low α) however is significant only in certain regions (NE Fennoscandia, Svalbard) that have very low precipitation today. α was 10–15% greater than present in S Europe and $P-E$ was 50–200 mm greater than present in most of S and E Europe, while $P-E$ was 50–250 mm less than present in most of NW Europe and in the high Alps.

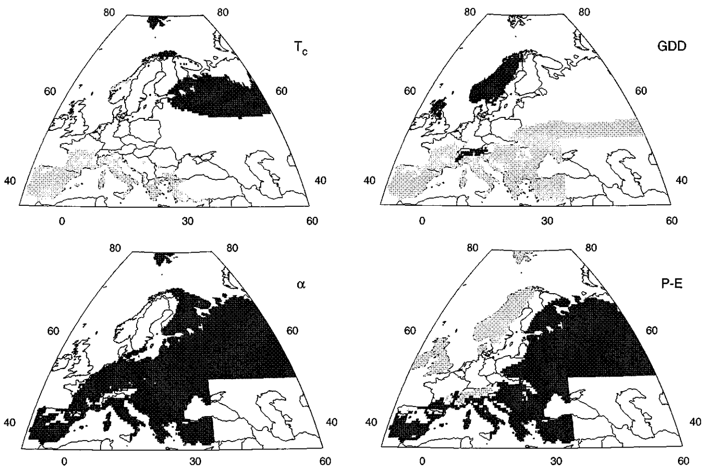

Fig. 5. Regions with significant climate anomalies, 6000 y BP minus present. *Dark shading* indicates regions with significant postive anomalies; *light shading* indicates regions with significant negative anomalies

Discussion

We have obtained these results using a form of statistical inverse modelling. The same general approach has been widely used in palaeoclimatology during the last two decades (see e.g. Webb and Clark 1977; Huntley and Prentice 1988; Guiot et al. 1989; Bonnefille et al. 1990; Prentice et al. 1991; Webb et al. 1993). Proxy data (in this case, pollen data) are used to infer anomalies of climate variables, which can then be compared with simulated palaeoclimate anomalies. We have overcome a number of persistent methodological problems with this approach by means of several innovations, including the use of lake-level data as a constraint on modern pollen analogue selection, the choice of climate variables that relate to the causal determinants of changes in vegetation and lakes, a correction for bias due to upward pollen transport in high-elevation sampling sites, and the use of a topographically sensitive interpolation method to construct palaeoclimate anomaly maps.

The results agree for the most part with the qualitative climatic inferences drawn by Huntley and Prentice (1993) and Prentice et al. (1996). The present work goes further by providing spatially coherent, quantitative estimates of 6000 y BP anomalies for the bioclimatic variables reflecting each of the major determinants of vegetation, namely winter cold, growing-sea-

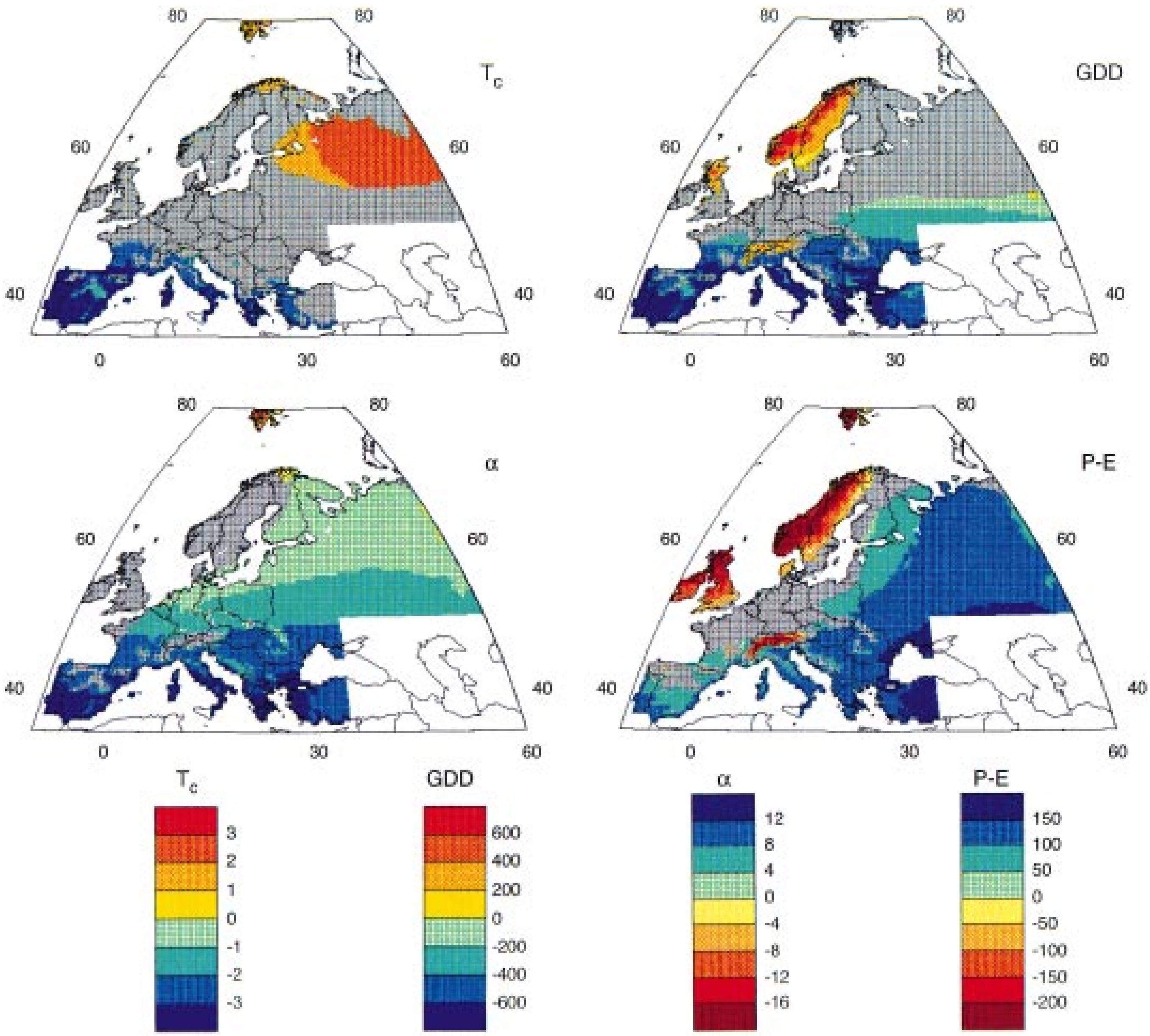

Fig. 6. Patterns of significant climate anomalies, 6000 y BP minus present: as Fig. 4, but regions shown as non-significant in Fig. 5 are shown by *grey shading*

son warmth, and moisture availability for vegetation (Woodward 1987; Prentice et al. 1992a). Furthermore, these results allow a firmy based reconstruction of palaeohydrological conditions, thanks to the existence of a strong spatial pattern of lake-level changes (Yu and Harrison 1995b; Harrison et al. 1996).

The inferred winter temperature anomaly patterns are consistent with the features inferred by Huntley and Prentice (1993) and Prentice et al. (1996). There is also a general correspondence between the pattern of *GDD* anomalies shown here and the pattern of July temperature anomalies reconstructed by Huntley and Prentice (1988) using a transfer function method, although Huntley and Prentice (1988) showed a greater area of summer warming in central Europe. The *GDD* anomaly map expresses the classical idea of the "climatic optimum" (thermal maximum) in the regions in which this was first identified (Scandinavia, the Alps and Britain), but it also provides a warning about the dangers of extrapolating climate change scenarios to different regions.

The variable α is an index of drought stress on vegetation, and is an important predictor of vegetation patterns in the Mediterranean regions where the drought season lasts several months. In the northern Mediterranean region, α is estimated here to have been ca 15% higher than the present. At values of $\alpha > 65\%$, open vegetation types (xerophytic woodland, shrubland or steppe) are replaced by forest (Prentice et al. 1992a). Present values of α in the Mediterranean region are generally $< 65\%$ (Huntley et al. 1995). The reconstructed α values for 6000 y BP are $> 65\%$, as would be expected given the predominance of temperate deciduous forests at that time (Prentice et al. 1996).

The anomaly map for $P-E$ highlights the west-east pattern in lake-level anomalies that was shown by Yu and Harrison (1995b) for N Europe. $P-E$ and α reflect different aspects of the water balance, and they diol not vary together. Other things being equal, changes in the absolute amount of precipitation will cause both indices to change in the same direction because E is ultimately limited by moisture supply, except in the wettest regions. On the other hand, changes in the *partitioning* of precipitation between evapotranspiration and runoff (for example, due to a change in the seasonal distribution of precipitation) will change the two indices in opposite directions (Prentice et al. 1992b). The broad similarity of the reconstructions for $P-E$ and α at 6000 y BP supports the conclusion of Guiot et al. (1993) that Holocene water-balance changes across Europe were driven primarily by changes in the amount of precipitation reaching different parts of the continent.

Huntley and Prentice (1988) did not correct for the "warm bias" (Table 3) in pollen-based temperature reconstructions from high elevations. Summer temperature anomalies >4 K, shown by Huntley and Prentice (1988) for high elevations in the Alps, may have been overestimated. Nevertheless, we show here that *GDD* anomalies in the Alps and surrounding regions were negative at low elevations and positive at high anomalies. *GDD* anomalies were also greatest at high elevations in NW Europe. The present results thus support the inference of Huntley and Prentice (1988), that environmental temperature lapse rates at 6000 y BP were less steep than present. The present results also indicate changes in the relationship between $P-E$ and elevation, with high-elevation sites in the Alps registering drier than present while the lowlands to the south were wetter than present. Simulating such aspects of the three-dimensional structure of palaeoclimate anomalies will be a challenge for high-resolution (regional) climate models.

Acknowledgements. Financial support for this work was provided by the Centre National de la Recherche Scientifique (CNRS), the Swedish Natural Science Research Council (NFR), the Royal Swedish Academy of Sciences (KVA) through their Soviet-Swedish Research Cooperation programme, the NOAA Climate and Global Change Program (Paleoclimatology) via a subcontract to S.P.H. from the University of Madison-Wisconsin, and the European Union (EU) through a grant under the Environment programme for the project "Climate Changes in Europe during the last two climatic cycles with emphasis on temperate post optimum evolution and entering into glaciation". We thank the European Pollen Data Base (EPD) contributors who have allowed us to use their data; the EPD is also supported by the EU Environment programme. The results have been archived in digital form at the National Geophysical Data Center (NGDC) at Boulder, Colorado, USA.

Appendix: lake level changes in humid climates

The water balance of a lake is given by

$$R+A(L)P=A(L)E_p+D+\Delta V \tag{A1}$$

where R is runoff from the catchment, $A(L)$ is lake area, P is precipitation, E_p is evaporation from the lake surface (equated potential evaporation), D is discharge (outflow), and ΔV is net change in lake volume (Szestay 1974; Street-Perrott and Harrison 1985). Runoff is given by

$$R=A(C)(P-E) \tag{A2}$$

where $A(C)$ is catchment area and E is actual evapotranspiration over the catchment. Dividing throug by basin (catchment and lake) area A, we have

$$(1-\theta)(P-E)+\theta P=\theta E_p+(D+\Delta V)/A \tag{A3}$$

where θ is the fraction of A that is occupied by the lake. D is a monotonically increasing function of lake level, which in turn is (except in very unusual topographies) a monotonically increasing function of $A(L)$.

We are interested in the equilibrium lake area, such that $\Delta V=0$. Linearizing D about the point of equilibrium we can write

$$D=Af(\theta-\theta_1) \tag{A4}$$

where f is the slope of a function relating discharge to θ, and θ_1 is the θ-intercept obtained by extrapolating this slope back to $D=0$. Equations A3 and A4 then give the equilibrium lake area ratio θ^* as

$$\theta^*=\frac{(P-E)+f\theta_1}{(E_p-E)+f} \tag{A5}$$

For closed lakes this simplifies to

$$\theta^*=(P-E)/(E_p-E) \tag{A6}$$

However, closed lakes can exist only if $E_p \geq P$, which is not so today over most of Europe.

Equations A5 and A6 can be used to examine the response of θ^* to climate change, and in particular to changes in $P-E$. $P-E$ may increase due to an increase in P or a decrease in E. Increasing P increases θ^* since P appears in the numerator only. Decreasing E increases both the numerator and the denominator, but because $\theta^*<1$, the effect on the numerator is dominant. Thus, both overflowing and closed lakes respond monotonically to changes in $P-E$.

Equation A5 shows that the level of an overflowing lake depends not only on climate, but also on aspects of the basin and outlet morphometry that govern how steeply discharge increases with lake area as expressed in the parameters f and θ_1. The larger f, the smaller the sensitivity to changes in climate. Experiments with a coupled catchment and lake hydrology model (Vassiljev et al. 1995) suggest that this sensitivity can vary considerably according to basin size and morphometry (Vassiljev and Harrison, unpublished results), such that not all overflowing lakes would be expected to show a measurable response to further increases in $P-E$. On the other hand many regions of Europe today have $E_p \approx P$, and may have supported lakes that were closed during times with less than present precipitation.

This analysis neglects the possible groundwater contribution to lake water inputs and outputs. In humid regions the groundwater contribution is usually small, and furthermore groundwater input will usually respond to climate changes in a qualitatively similar way to $P-E$.

References

Bonnefille R, Roeland JC, Guiot J (1990) Climatic reconstructions for the last 40000 years in East Africa. Nature 346:347–349

Caudill M, Butler C (1992) Understanding neural networks. Vol. 1. Basic networks. MIT Press, 309 pp

COHMAP Members (1988) Climatic changes of the last 18000 years: observations and model simulations. Science 241:1043–1052

Evans S, Trevisan M (1995) A soil water-balance 'bucket' model for paleoclimatic purposes 2. Model application to late Holocene climate. Ecol Model 82:131–138

Guiot J (1990) Methodology of paleoclimatic reconstruction from pollen in France. Palaeogeogr, Palaeoclimatol, Palaeoecol 80:49–69

Guiot J, Pons A, de Beaulieu JL, Reille M (1989) A 140000-year climatic reconstruction from two European pollen records. Nature 338:309–313

Guiot J, Harrison SP, Prentice IC (1993) Reconstruction of Holocene precipitation patterns in Europe using pollen and lake-level data. Quat Res 40:139–149

Guiot J, Cheddadi R, Prentice IC, Jolly D (1996) A method of biome and land surface mapping from pollen data: application to Europe 6000 years ago. Paleoclimates 1:311–324

Harrison SP, Yu G, Tarasov PE (1996) The Holocene lake-level record from Eurasia. Quat Res 45:138–159

Huntley B (1994) Late Devensian and Holocene palaeoecology and palaeoenviroments of the Morrone Birkwoods, Aberdeenshire, Scotland. J Quat Sci 9:311–336

Huntley B, Birks HJB (1983) An atlas of past and present pollen maps for Europe 0–13000 years ago. Cambridge University Press, 667 pp

Huntley B, Prentice IC (1988) July temperatures in Europe from pollen data, 6000 years before present. Science 241:687–690

Huntley B, Prentice IC (1993) Holocene vegetation and climates of Europe. In: Wright HE Jr, Kutzbach JE, Webb T III, Ruddiman WF, Street-Perrott FA, Bartlein PJ (eds) Global climates since the last glacial maximum. University of Minnesota, Minneapolis, pp 136–168

Huntley B, Berry PM, Cramer W, McDonald AP (1995) Modelling present and potential future ranges of some European higher plants using climate response surfaces. J Biogeogr 22:967–1001

Kutzbach JE, Street-Perrott FA (1985) Milankovitch forcing of fluctuations in the level of tropical lakes from 18 to 0 ky BP. Nature 317:130–134

Leemans R, Cramer W (1991) The IIASA data base for mean monthly values of temperature, precipitation and cloudiness on a global terrestrial grid. RR-91-18. International Institute for Applied Systems Analysis, Laxenburg

Overpeck JT, Webb T III, Prentice IC (1985) Quantitative interpretation of fossil pollen spectra: dissimilarity coefficients and the method of modern analogs. Quat Res 23:87–108

Peterson GM (1983) Holocene vegetation and climate in the western USSR. PhD Thesis, University of Wisconsin, Madison, USA

Prentice IC, Bartlein PJ, Webb T III (1991) Vegetation and climate changes in eastern North America since the last glacial maximum. Ecology 72:2038–2056

Prentice IC, Cramer W, Harrison SP, Leemans R, Monserud RA, Solomon AM (1992a) A global biome model based on plant physiology and dominance, soil properties and climate. J Biogeogr 19:117–134

Prentice IC, Guiot J, Harrison SP (1992b) Mediterranean vegetation, lake levels and palaeoclimate at the Last Glacial Maximum. Nature 360:658–670

Prentice IC, Guiot J, Huntley B, Jolly D, Cheddadi R (1996) Reconstructing biomes from palaeoecological data: a general method and its application to European pollen data at 0 and 6 ka. Clim Dyn 12:185–194

Street-Perrott FA, Harrison SP (1985) Lake levels and climate reconstruction. In: Hecht AD (ed) Paleoclimate analysis and modelling. Wiley, Chichester, pp 291–340

Street-Perrott FA, Marchand DS, Roberts N, Harrison SP (1989) Global lake-level variations from 18000 to 0 years ago: a palaeoclimatic analysis. DOE/ER/60304-H1 TR046, US Department of Energy

Szestay K (1974) Water balance and water level fluctuations of lakes. Hydrol Sci Bull 19:73–84

Tarasov PE, Harrison SP, Saarse L, Pushenko MYa, Andreev AA, Aleshinskaya ZV, Davydova NN, Dorofeyuk NI, Efremov YuV, Khomutova VI, Sevastyanov DV, Tamosaitis J, Uspenskaya ON, Yakushko OF, Tarasova IV (1994) Lake status records from the former Soviet Union and Mongolia: Data base documentation. NOAA Paleoclimatology Publications Series Report 2, 274 pp

Vassiljev J, Harrison SP, Haxeltine A (1995) Recent lake-level and outflow variations at Lake Viljandi, Estonia: validation of a coupled lake-catchment modelling scheme for climate change studies. J Hydrol 170:63–77

Webb T III, Clark DR (1977) Calibrating micropaleontological data in climatic terms: a critical review. Ann New York Acad Sci 288:93–118

Webb T III, Bartlein PJ, Harrison SP, Anderson KH (1993) Vegetation, lake-levels, and climate in eastern North America since 12000 y BP. In: Wright HE Jr, Kutzbach JE, Webb T III, Ruddiman WF, Street-Perrott FA, Bartlein PJ (eds) Global climates since the last glacial maximum. University of Minnesota Press, Minneapolis, pp 415–467

Woodward FI (1987) Climate and plant distribution. Cambridge University Press, Cambridge, UK

Wright HE Jr, Kutzbach JE, Webb T III, Ruddiman WF, Street-Perrott FA, Bartlein PJ (eds) (1993) Global climates since the last glacial maximum. University of Minnesota Press, Minneapolis, 569 pp

Yu G, Harrison, SP (1995a) Lake status records from Europe: Data base documentation. NOAA Paleoclimatology Publications Series Report 3, 451 pp

Yu G, Harrison SP (1995b) Lake status changes in northern Europe during the Holocene. Boreas 24:260–268